RSC Advances

REVIEW

View Article Online
View Journal | View Issue

Cite this: *RSC Adv.*, 2025, **15**, 26537

One-pot production of bio-based 2-methyltetrahydrofuran and 2,5-dimethyltetrahydrofuran: a review of heterogeneous catalytic approaches

Ngan Nguyen Le,[ab] Ngan Tuan Nguyen,[c] Hoang Long Ngo,[c] Thanh Tung Nguyen[c] and Cong Chien Truong *[c]

The valorisation of biomass into value-added products plays an important role in the establishment of sustainable chemistry and a circular economy. Leveraged as renewable feedstocks, furfural (FF), 5-hydroxymethyl furfural (5-HMF), carbohydrates, and lignocellulose can be transformed into bio-based 2-methyltetrahydrofuran (2-MTHF) and 2,5-dimethyltetrahydrofuran (2,5-DMTHF) under specific conditions. This article presents a comprehensive discussion of the one-pot manufacture of renewable 2-MTHF and 2,5-DMTHF through the heterogeneous catalytic cascade of hydrodeoxygenation–hydrogenation and hydrodeoxygenation-transfer hydrogenation using H_2 and alcohols as green reductants. Particularly, this review provides a thorough understanding of catalyst design, reaction optimization, operation mode (batchwise *vs.* continuous flow), catalyst reusability, and mechanistic pathways to access the target products. Furthermore, an elaborate analysis of the outlook and constraints related to these straightforward and eco-friendly approaches is also presented.

Received 16th May 2025
Accepted 7th July 2025

DOI: 10.1039/d5ra03460d

rsc.li/rsc-advances

[a]*Institute of Applied Science and Technology, School of Technology, Van Lang University, Ho Chi Minh City, Vietnam*

[b]*Faculty of Applied Technology, School of Technology, Van Lang University, Ho Chi Minh City, Vietnam*

[c]*NTT Hi-Tech Institute, Nguyen Tat Thanh University, 300A Nguyen Tat Thanh Street, Ward 13, District 4, Ho Chi Minh City, Vietnam. E-mail: tcchien@ntt.edu.vn*

Ngan Nguyen Le

Ngan Nguyen Le received his PhD in Materials Science from the University of Science, Vietnam National University, Ho Chi Minh City, in 2021. He was formerly the Head of the Laboratory for Characterization of Nanomaterials – Devices & Applications at the Institute for Nanotechnology, Vietnam National University Ho Chi Minh City. In 2024, he transitioned to working as a research expert at the Institute of Applied Science and Technology, Van Lang University. His research interests include materials science, nanomaterials, nanocomposites, artificial intelligence and inkjet printing. He is the author and co-author of more than 20 publications in peer-reviewed journals, one book chapter published by Academic Press and two patents. He has received two Certificates of Merit from the Minister of Education and Training of Vietnam and one National Award, and has been recognized as an innovator with nationwide effectiveness and applicability.

Ngan Tuan Nguyen

Ngan Tuan Nguyen obtained his master's degree from the University of Science, Vietnam National University, Ho Chi Minh City, in 2024. He is working as a researcher at the NTT Hi-Tech Institute, Nguyen Tat Thanh University, Ho Chi Minh City, Vietnam. His research focuses on biomass conversion, application of biochar, porous structured materials, and various types of polymers in environmental remediation and capacitive deionization (CDI) technology.

1. Introduction

The serious consequences of global warming and the excessive use of fossil resources have sparked greater interest in tapping into renewable resources in recent years.[1,2] In this context, biomass is regarded as one of the most prominent alternatives to petrochemicals thanks to the large reserves, worldwide accessibility, and carbon neutrality. Attractively, the valorisation of raw biomass materials (cellulose and lignocellulose) into valuable fuels, commodity chemicals, materials, and intermediates not only enhances the efficient management of natural resources and energy security but also alleviates global threats of escalating CO_2 emissions and depletion of fossil reserves.[3,4]

Among biomass-derived key platform molecules, furfural (FF) and 5-hydroxymethylfurfural (5-HMF) are recognized as prime building blocks for a broad spectrum of pharmaceuticals, agrochemicals, plastics, and solvents.[5,6] Specifically, a plethora of important downstream chemicals can be established from these two furanic molecules through a variety of chemical reactions, including oxidation, hydrogenation, etherification, esterification, hydrogenolysis, hydrodeoxygenation, condensation, amination, and tandem processes. Representatively, bio-based 2-methyltetrahydrofuran (2-MTHF) and 2,5-dimethyltetrahydrofuran (2,5-DMTHF), which are endowed with a saturated furan ring, serve as potential additives in the fuel market as they offer excellent advantages of high storage stability, high energy density, low volatility, water immiscibility, and excellent compatibility with gasoline.[7] As compared to conventional petrol, ethanol and isooctane, the distinct beneficial characteristics of 2-MTHF and 2,5-DMTHF for practical application as fuel additives are summarized in Table 1.[8–10] Apart from this salient practicality, 2-MTHF and 2,5-DMTHF are exploited as eco-friendly solvents across various domains, including organo-/bio-catalysis, organometallic chemistry, and extraction.[11–13] In terms of degradability, these biogenic cyclic ethers are readily degraded owing to the furan ring opening upon exposure to sunlight. Importantly, the hydrodeoxygenation of 2-MTHF and 2,5-DMTHF provides a feasible means of producing biogenic dienes and alkanes.[14,15] As summarized in Table 2, various petroleum-free feedstocks for producing 2-MTHF and 2,5-DMTHF are described.

Given the tremendous demand for bio-based 2-MTHF and 2,5-DMTHF as well as several limitations (*i.e.*, substrate availability, arduous recovery of homogeneous catalyst systems), this review provides a systematic and comprehensive overview of the straightforward manufacture of these cyclic ethers from FF, 5-HMF, carbohydrates, and lignocellulose through the heterogeneous catalytic cascade of hydrodeoxygenation–hydrogenation and hydrodeoxygenation-transfer hydrogenation, using H_2 and alcohols as the hydrogen donor, respectively (Scheme 1).

For this purpose, particular emphasis will be placed upon the rational design of supported noble/non-noble metal catalysts and reaction optimization to ensure the high productivity of 2-MTHF and 2,5-DMTHF. Furthermore, catalyst reusability and continuous-flow implementation, which are of industrial importance, are also elaborated. To the best of our knowledge,

Hoang Long Ngo

Dr Hoang Long Ngo obtained his PhD degree from the Korea University of Science and Technology (UST) in 2020. Currently, he is working as a researcher at the NTT Hi-Tech Institute, Nguyen Tat Thanh University, Ho Chi Minh City, Vietnam. His research primarily focuses on environmental remediation, porous materials such as MOFs derived from PET, biochar from biomass, various polymer membranes, extraction of organic compounds, and organic synthesis.

Thanh Tung Nguyen

Dr Thanh Tung Nguyen is a researcher at NTT Hi-Tech Institute, Nguyen Tat Thanh University, Ho Chi Minh City, Vietnam. He obtained his PhD degree in industrial technology from Korea University of Science and Technology (UST) in 2020. His research interests include biomass utilization, composite materials, catalysis, and wastewater treatment. His current research focuses on the valorization of biomass and bio-waste into value-added products, including lignin-derived chemicals and carbon-based materials for organic synthesis and wastewater treatment.

Cong Chien Truong

Dr Cong Chien Truong obtained his PhD degree from the Korea University of Science and Technology (UST) in 2020. Currently, he is working as a researcher at the NTT Hi-Tech Institute, Nguyen Tat Thanh University, Ho Chi Minh City, Vietnam. His research interests include homogeneous/heterogeneous catalyst design for the divergent synthesis of heterocyclic frameworks as well as the valorization of carbon dioxide and biomass into value-added products.

Table 1 Comparison of the properties of 2-MTHF and 2,5-DMTHF

Properties	Petrol	Isooctane	Ethanol	2-MTHF	2,5-DMTHF
Lower heating value (MJ kg^{-1})	42.9	44.2	26.8	32.7	38.3
Heat of vaporization (kJ kg^{-1})	373	—	912	375	348
Research octane number (RON)	90–99	100	109	86	119
Motor octane number (MON)	86	100	90	73	82
Stoichiometric air/fuel ratio	14.46	15.10	9	11.23	11.73
SO_2 formation normalized (wt%)	7.1	—	—	—	—
NO_x formation (ppm)	1.72	—	—	—	—
Boiling point (°C)	25–215	99.2	78	80.2	91
Density at 20 °C (g cm^{-3})	0.745	0.691	0.791	0.863	0.83
Viscosity at 40 °C (mm^2 s^{-1})	0.4–0.8	0.65	0.79	0.66	0.47
Water solubility (% v/v)	Negligible	Not miscible	Miscible	12.1	0.26

Table 2 Production of 2-MTHF and 2,5-DMTHF from bioderived feedstocks

	Starting materials	
Products	Biomass-derived chemicals	Raw biomass
2-MTHF	FF, 2-methylfuran (2-MF), levulinic acid (LVA), γ-valerolactone (GVL), 1,4-pentanediol	Xylose
2,5-DMTHF	5-HMF, 2,5-dimethylfuran (2,5-DMF), 2,5-hexanediol (2,5-HDL), 2,5-hexanedione (2,5-HDE)	Glucose, inulin, sucrose, cellulose

there are no accounts of the one-pot production of bio-based 2-MTHF and 2,5-DMTHF documented in the literature. Therefore, this article is exclusively pitched at filling the knowledge gap between catalyst performance and mechanistic insights into the strategy of hydrodeoxygenation–hydrogenation and hydrodeoxygenation-transfer hydrogenation, providing valuable references for both scholars and engineers in the mass production of 2-MTHF and 2,5-DMTHF.

2. Catalytic hydrodeoxygenation–hydrogenation cascade of FF and 5-HMF

2.1. Preparation of 2-MTHF from FF

As shown in Scheme 2, the reductive transformation of FF into 2-MTHF can take place through multiple reactions (hydrogenation and deoxygenation) with the involvement of various intermediates. Generally, the establishment of 2-MTHF can occur *via* two fundamentally distinct routes. The first approach starts with the hydrogenation of the aldehyde (–CHO) group of FF to give the FAL intermediate, followed by the formation of 2-MF or THFAL, and ultimately, the production of 2-MTHF. Meanwhile, the second route is associated with the hydrodeoxygenation of FF towards 2-MF, followed by the hydrogenation of the furan ring to generate 2-MTHF. Therefore, the proper selection of the catalyst and reaction conditions for selective hydrodeoxygenation–hydrogenation of FF is crucial; otherwise, undesired products can be obtained. This section will describe the performance of different supported mono-/multi-metallic catalysts for the production of 2-MTHF with respect to both the nature of the catalysts and the reaction parameters.

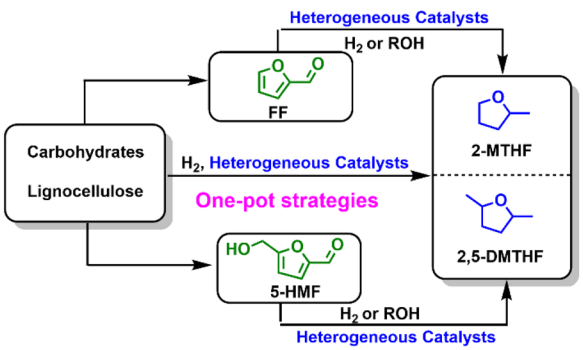

Scheme 1 One-pot production of 2-MTHF and 2,5-DMTHF from biomass materials over heterogeneous catalysts.

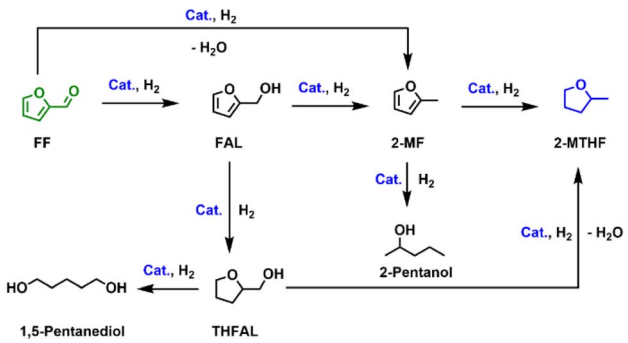

Scheme 2 Reaction pathway for the hydrodeoxygenation–hydrogenation cascade of FF towards 2-MTHF.

Recently, transition metal phosphides have emerged as low-cost and efficient alternatives to precious metal-based catalysts in a wide range of reactions (hydrogenation, hydrodeoxygenation, hydrodesulfurization, *etc.*) owing to their tuneable structures, high reactivity, and excellent durability.[16,17] To enhance the catalytic performance, ultrasmall active nickel phosphide nanoparticles (Ni_2P) are generally impregnated on large-surface-area carriers. Considering the benefits of porous carbon materials derived from the pyrolysis-carbonization of MOFs, Li *et al.* described the construction and performance of a well-defined organodiphosphonate MOF-derived Ni-P@C catalyst for the hydrodeoxygenation–hydrogenation of FF.[18] Comprehensive catalyst characterizations revealed that the graphitized carbon coating of Ni-P@C not only reduces the temperature for the formation of the Ni_2P active phase but also inhibits the agglomeration of these particles, efficiently boosting the stability and reusability of Ni-P@C during the hydrodeoxygenation–hydrogenation. Accordingly, the highest 2-MTHF yield of 72.2% was provided when the reaction of FF with 20 bar H_2 was carried out at 260 °C and 8 h.

Inspired by the deployment of nitrogen-doped carbon materials to stabilize active species (single metal atoms, metal complex, and metal NPs) for the oxidation and hydrogenation reaction, Han *et al.* proposed a facile pyrolysis strategy to attain a nitrogen-doped carbon-stabilized Co NPs and single Co atom catalyst (1.07 wt% Co@NC).[19] It was discovered that the designed catalyst, prepared by annealing a mixture of folic acid, α-cellulose, and $Co(NO_3)_2 \cdot 6H_2O$ at 600 °C under an argon atmosphere, possessed a high surface area and featured both single Co atoms and Co NPs. A series of controlled experiments and DFT calculations on the hydrodeoxygenation–hydrogenation of acetophenone towards ethylcyclohexane over the Co@NC catalyst disclosed that the single Co atoms served as Lewis acid centres in the activation of C=O/C–OH bonds and the benzene ring, while metallic Co NPs took part in the generation of reactive hydrogen species from H_2. Thanks to the remarkable synergism of these active components, FF and 5-HMF were converted to 2-MTHF and 2,5-DMTHF in excellent yields (>97%), respectively, under mild conditions of 10 bar H_2 and 150 °C.

During the reductive transformation of FF over a variety of carbon-supported Pd catalysts, Date and coworkers reported that the predominant establishment of 2-MTHF could be accomplished by controlling the Pd particle size.[20] In this context, different reductants (*i.e.*, $NaBH_4$, HCHO, and H_2) were applied during the catalyst preparation, wherein the corresponding Pd crystallite size was arranged in the order of: 4 wt% Pd_{5H}/C (5% H_2 + 95% N_2) < 4 wt% Pd_{NaBH_4}/C < 4 wt% Pd_{50H}/C (50% H_2 + 50% N_2) < 4 wt% Pd_{100H}/C (100% H_2) < 4 wt% Pd_{HCHO}/C. In line with this, 4 wt% Pd_{NaBH_4}/C, which achieved a small Pd particle size (~4.8 nm) due to the incorporation of boron atoms into the inner lattices of Pd–Pd, delivered the highest 2-MTHF selectivity of 40% when FF was treated with 34.5 bar H_2 at 220 °C in 2-propanol. Besides, the presence of Pd-B species also helped to suppress the formation of FAL and 1,5-pentanediol, thereby enhancing the selectivity for 2-MTHF. Additional recycling tests proved that spent 4 wt% Pd_{NaBH_4}@C was able to maintain the initial reactivity after regeneration (air calcination and H_2 reduction). Later, an array of phosphate-supported single atom and NPs of Pd, including $Pd_{1+NP}/AlPO_4$, Pd_{1+NP}/BPO_4, $Pd_{1+NP}/Al(PO_3)_3$, and $Pd_{1+NP}/Y(PO_3)_3$, was tested for the hydrodeoxygenation–hydrogenation model at room temperature.[21] Of these, $Pd_{1+NP}/AlPO_4$ enabled 100% conversion of FF and 5-HMF into 2-MTHF and 2,5-DMTHF at selectivity of 70.8% and 56%, respectively, after reacting for 12 h in THF. Exhaustive characterization and theoretical calculations disclosed that *in situ* heterolysis of H_2 at the Pd single atom–$AlPO_4$ interface generated the frustrated Lewis H^+–H^- pairs, which expedited the cleavage of the C–OH bond in FAL to render 2-MF. Meanwhile, H atoms on the surface of the Pd NPs promoted the hydrogenation of 2-MF into 2-MTHF.

Motivated by the practicality of heterogeneous Ir–Ni bimetallic catalyst systems in the hydrogenation of α,β-unsaturated aldehydes, the Rode research group fabricated a collection of carbon-supported Ir–Ni bimetals using two methods, co-impregnation (Ir–Ni@C_{cp}, Ir = 4 wt%; Ni = 7.5, 10, 17.5, 25 wt%) and sequential addition (Ir–Ni@C_{sa}, Ir = Ni = 4%), to catalyse the one-pot formation of 2-MTHF.[22] Through a set of control experiments and structural analyses, the synergistic impacts of Ir phases (Ir^0 + IrO_2), Ni species (Ni^0 + NiO), the presence of oxygen vacancies, moderate acid sites (NiO + IrO_2), and the Brønsted acidity of carbonaceous support on the yield of 2-MTHF were determined for all designed catalysts. Accordingly, 2-MTHF selectivity reached 63% over 4 wt% Ir–10 wt% Ni@C_{cp} and 74% over 4 wt% Ir–4 wt% Ni@C_{sa} after 5 hours of reaction at 220 °C in 2-propanol. Regarding the recyclability, the recovered 4 wt% Ir–4 wt% Ni@C_{sa} catalyst could be reused for three consecutive runs with only a marginal loss of reactivity. Further trials using two intermediates (FAL and 2-MF) as substrates demonstrated that 2-MTHF could be afforded under established conditions, whereas THFAL did not yield the target product.

Afterwards, Huang and coworkers investigated the production of 2-MTHF by using carbon-supported Co NPs with varying contents of Zn dopant (0.38, 1.07, and 2.74 wt%), prepared through the pyrolysis of Zn–Co-ZIF precursors.[23] Supported by in-depth structural characterizations (XRD, SEM, TEM, XPS, and H_2-TPR), it was verified that Zn was coordinated with N species in the carbon support, boosting the electron transfer from the Zn-doped carbon to metallic Co particles. Furthermore, the doped Zn was deemed beneficial to advocating the H_2 dissociation and lowering the diffusion barrier of the H atom, thereby stimulating the rate of hydrogenation reactions. Besides, data from *in situ* FT-IR and computational calculations pointed out that the presence of doped Zn species not only efficiently optimized the adsorption of the substrates/intermediates in the hydrogenation but also reduced the potential barriers of C–OH bond cleavage in the hydrodeoxygenation. Consistent with profound impacts of Zn doping on the electronic structure and catalytic activity of Zn–Co/NC samples, the yields of 2-MTHF under optimized conditions (10 bar H_2, 200 °C, 8 h) were ranked as follows: 2.74 wt% Zn–Co/NC (79.2%) < 1.07 wt% Zn–Co/NC (85.5%) < 0.38 wt% Zn–Co/NC (93.8%). On top of that, 0.38 wt% Zn–Co/NC showed no changes

in the structure, morphology, and original catalytic activity after several runs.

In another study reported by Yang and coworkers, the reactivity of various HY zeolite-impregnated bimetallic Cu–Pd catalysts (Cu–Pd/HY) towards 2-MTHF production was thoroughly evaluated.[24] It is well known that the size and dispersion of metal particles, as well as the metal alloying in Cu–Pd/HY series, are closely linked to the Cu/Pd mass ratio and significantly determine the reaction outcomes. Correspondingly, the yield of 2-MTHF was arranged in the order of 10 wt% Cu–1 wt% Pd/HY (0%) < 10 wt% Cu–9 wt% Pd/HY (25.8%) < 10 wt% Cu–3 wt% Pd/HY (55.2%) < 10 wt% Cu–7 wt% Pd/HY (73.3%) < 10 wt% Cu–5 wt% Pd/HY (83.1%) after 3 hours of reaction at 220 °C with 30 bar H_2 in *n*-heptane. This rank was rationalized by the fact that the ideal Cu/Pd ratio in 10 wt% Cu–5 wt% Pd/HY not only promoted the reduction of 2-MF intermediate into 2-MTHF but also suppressed the competitive formation of THFA from FF. In addition to the participation of Cu–Pd active sites, the preponderance of moderate and strong acid sites in the HY support appreciably contributed to the hydrodeoxygenation activity of 10Cu–5Pd/HY as well. Additionally, a set of control experiments and *in situ* DRIFT analysis disclosed that the conversion of FF to 2-MTHF followed the main sequence of: (i) the –CHO group of FF is adsorbed at the Cu active sites and reacts with adsorbed-dissociated hydrogen atoms to deliver FAL; (ii) the $–CH_2OH$ group of FAL is adsorbed at the Cu^+ sites, and the acidity of the HY support promotes the breaking of C–OH bond so as to deliver 2-MF; and (iii) the 2-MF molecule is adsorbed on the catalyst surface and subsequently hydrogenated into 2-MTHF.

Trimetallic Cu–Ni–Re decorated on Hβ zeolite catalyst (15 wt% Cu–4 wt% Ni–4 wt% Re/Hβ) could mediate 100% conversion of FF into 81% selectivity of 2-MTHF under optimized conditions (30 bar H_2, 240 °C, 2 h) in *n*-hexane.[25] The outperformance of 15 wt% Cu–4 wt% Ni–4 wt% Re/Hβ over benchmark catalysts (*i.e.*, 15 wt% Cu/Hβ, 4 wt% Ni/Hβ, 4 wt% Re/Hβ, 15 wt% Cu–4 wt% Ni/Hβ, 15 wt% Cu–4 wt% Re/Hβ, 4 wt% Ni–4 wt% Re/Hβ, and 15 wt% Cu–4 wt% Ni–4 wt% Re/SiO_2) was accredited to: (i) the high density of moderately strong acid sites on the Hβ support; and (ii) the synergism of metals during the adsorption-dissociation of H_2, adsorption of reactant/intermediates, hydrodeoxygenation, and hydrogenation. Regarding durability, the spent 15 wt% Cu–4 wt% Ni–4 wt% Re@Hβ catalyst showed a slight reduction in activity after four recycles due to the leaching of metals and deposition of carbonaceous materials on active sites. In this study, ATR-IR spectroscopy was employed to detect the adsorption state as well as to elucidate the reaction pathway, from which the formation of 2-MTHF is specified as follows: (i) H_2 is adsorbed and dissociated at the Cu and Ni sites; (ii) FF is adsorbed at the Cu and Ni sites through the –CHO group, which is subsequently hydrogenated to FAL; (iii) the adsorption of the $–CH_2OH$ group of FAL takes place at the acid sites of Hβ, followed by hydrogenolysis to form 2-MF at the Cu and Re sites; (iv) the reduction of 2-MF to produce 2-MTHF proceeds at the Cu and Ni sites.

Apart from organic solvents, the metal-catalysed hydrodeoxygenation–hydrogenation cascade of FF was also conducted in water. For example, a maximum 2-MTHF yield of 35.6% was attained when the bimetallic Cu–Ni supported on SBA-15 (Cu–Ni/SBA-15; 10 wt% Ni, Ni/Cu molarity = 2) was used for the transformation of FF with 40 bar H_2 at 160 °C in water.[26] In this case, the majority of the product was cyclopentanone rather than 2-MTHF, which accounted for the unsatisfactory yield. Meanwhile, 2-MTHF (26.9%) and unidentified products (48.2%) were concomitantly yielded through the one-pot, two-stage thermal treatment of FF under 60 bar H_2 in water over a bimetallic 4 wt% Ir–7.8 wt% ReO_x/SiO_2 catalyst.[27] Similarly, 2-MTHF was obtained in low yields (max. 10.31%) when carbon-supported noble metals (5 wt% M/C; M = Pt, Pd, and Ru) were used for the hydrodeoxygenation–hydrogenation of FF in the water, even under harsh conditions (80 bar H_2, 175 °C).[28]

To summarize, the proper selection of active catalysts and reaction parameters holds the key to the straightforward synthesis of 2-MTHF from FF. In most examples, the reaction mechanism is established through the pathway of FF → FAL → 2-MF → 2-MTHF, wherein the cooperative engagement of metals and acid sites of supports are deemed critically vital.

2.2. Preparation of 2,5-DMTHF from 5-HMF

Similar to FF, the catalytic conversion of 5-HMF to 2,5-DMTHF in the presence of H_2 takes place through two principal pathways (Scheme 3). The first route is associated with the production of 5-MF through the hydrodeoxygenation of the $–CH_2OH$ group of 5-HMF, whereas the reduction of the –CHO moiety of 5-HMF to produce the BHMF intermediate occurs first in the second route. Consequently, the proper selection of metal catalysts and reaction variables for selective hydrodeoxygenation–hydrogenation of 5-HMF is crucial; otherwise, the distribution of undesired products would become dominant. This section will provide details about the performance of different supported mono-/multi-metallic catalysts for the synthesis of 2,5-DMTHF in terms of catalyst nature and reaction parameters.

It is well established that the size and dispersion of metal nanoparticles (NPs), the strength of metal–support interaction, and the acid–base property of TiO_2-supported metal NPs are greatly influenced by the nature of the TiO_2 phase.[29] Driven by this fact, Przydacz *et al.* investigated a collection of 10 wt% Ni/TiO_2 samples, which were fabricated from nickel nitrate and various commercial TiO_2 powders encompassing pure anatase

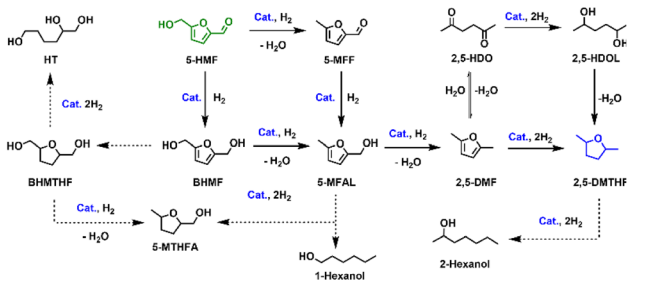

Scheme 3 Reaction pathway for the hydrodeoxygenation–hydrogenation cascade of 5-HMF towards 2,5-DMTHF.

(UV100 and PC500) or anatase-rutile mixed phase (P25 and P90) *via* incipient wetness impregnation-reduction method to catalyse the hydrodeoxygenation–hydrogenation of 5-HMF.[30] The textural characterizations (Table 3) indicated that the properties of TiO_2 pivotally determined the particle size of the Ni species, the strength of the Ni–TiO_2 interaction and the acidity, consequently exerting a momentous impact on the catalytic performance of Ni/TiO_2 samples. In this context, the 2,5-DMTHF selectivity at complete 5-HMF conversion was ranked in the order of: Ni/TiO_2-PC500 < Ni/TiO_2- UV100 < Ni/TiO_2-P90 < Ni/TiO_2-P25 under experimental conditions (30 bar H_2, 220 °C, 2 h) in 1,4-dioxane. Herein, the large amount of 2,5-DMTHF as witnessed in rutile-encompassing catalysts came from: (i) the strong NiO_x–TiO_2 interaction; (ii) the high concentration of surface Lewis acid centres; and (iii) large Ni crystallites. Therefore, the adsorption–desorption of hydrogen was facilitated, and the transformation of 5-HMF to 2,5-DMTHF is suggested to take place concomitantly through both the 5-MFF and BHMF routes. Meanwhile, small Ni particles in anatase-based materials strongly adsorbed but partly restricted the desorption of hydrogen, favoring the formation of 2,5-DMF rather than 2,5-DMTHF through the 5-MFF pathway (Scheme 3).

Adopting the mesoporous SBA-15 material to impregnate Ni NPs, Chen *et al.* successfully designed 15 wt% Ni/SBA-15 to promote the production of 2,5-DMTHF.[31] Through proper regulation of the reaction time and temperature, it is possible to induce 100% conversion of 5-HMF towards 97% selectivity of 2,5-DMTHF after 10 h at 180 °C and 30 bar H_2 in 1,4-dioxane. Otherwise, 2,5-DMF (70.5%) and a complex mixture (2,5-DMTHF + BHMF + MFOL = 21.1%) were simultaneously yielded within 0.5 h. Unsurprisingly, increasing the reaction temperature (>180 °C) and/or shortening the reaction timespan (<10 h) were detrimental to the outcome of 2,5-DMTHF. Herein, the remarkable activity of Ni/SBA-15 to facilitate both the hydrogenolysis and furan ring hydrogenation can be accredited to the presence of Ni^0 particles confined in the mesopores, and the kinetic study revealed that 5-HMF conversion probably followed the sequence of 5-HMF → 5-MFF → 5-MFAL → 2,5-DMF → 2,5-DMTHF. In the recycling test, 15 wt% Ni/SBA-15 encountered progressive catalytic deactivation during three consecutive runs, even when the recovered catalyst was subjected to stepwise thermal post-treatment (calcination at 500 °C and reduction at 550 °C) in every cycle. Under such circumstances, both 5-HMF conversion and the total yield of identified products diminished in line with the number of recycles, which was attributed to the accumulation of organic species over the surface-active sites rather than the aggregation of Ni NPs and/or degradation of mesostructured SBA-15.

In another study conducted by Zhang and coworkers, 51.1% selectivity for 2,5-DMTHF was acquired under the catalysis of Ni NPs decorated on sucrose-derived hydrothermal carbon spheres calcined at 350 °C (unreduced 5 wt% Ni/HC-350) when the reaction of 5-HMF was executed in 1,4-dioxane for 10 h at 200 °C and 15 bar H_2.[32] Reversely, 5 wt% Ni/HC samples that were subjected to calcination at high temperatures (>350 °C) or thermal pretreatment in H_2 (450 °C) showed a preference for 2,5-DMF and 2,5-BHMF under identical conditions. This is attributed to the majority of small crystallite sized Ni and the synergistic Ni–NiO system (metal–acid bifunctional sites) as witnessed in unreduced 5 wt% Ni/HC-350, which is strongly dependent on the metal loading, calcination temperature, and the absence of a reduction step.

To achieve 2,5-DMTHF at mild temperature, Kong *et al.* introduced a convenient two-stage procedure to prepare a Ni NPs-embedded nickel phyllosilicate catalyst (NiSi-PS, 36.1 wt% Ni).[33] A combination of structural characterizations (N_2 adsorption, XRD, H_2-TPR, NH_3-TPD, and Py-IR) confirmed that the bifunctional NiSi-PS catalyst was conferred with a fibrous structure, a large surface area (352.5 $m^2\ g^{-1}$), a uniform dispersion of Ni NPs, a high surface metallic density (0.19 mmol g_{cat}^{-1}) and a significant proportion of Lewis acid sites (1.84 μmol $NH_3\ g_{cat}^{-1}$), which surpassed those of conventional silica-impregnated Ni counterparts (Ni/SiO_2, Ni = 20 and 36 wt%). In essence, the remnant nickel phyllosilicate structure after H_2 reduction served as a carrier for both the metal (Ni^0 particles) and the proximal Lewis acid site (coordinatively unsaturated Ni^{2+} sites), synergistically benefiting the tandem reaction of 5-HMF. As a result, the high-performance NiSi-PS catalyst enabled an 89.7% yield and selectivity for 2,5-DMTHF under moderate conditions (15 bar H_2, 150 °C, 8 h) in 1,4-dioxane, whereas Ni/SiO_2 and other benchmark catalysts (Raney-Ni or 20 wt% Ni/ZrO_2) failed to achieve the same result. Even with a prolonged timespan of 20 h, another reference catalyst (20 wt% Ni/Al_2O_3) only gave 2,5-DMTHF with 72.4% selectivity at its best. In addition to 5-HMF, the cascade reaction catalysed by NiSi-PS was also applicable to 5-MFF and FF under milder conditions (15 bar H_2, 150 °C, 3 h), producing 2,5-DMTHF and 2-MTHF in 76.9% and 78.3% yields, respectively. Despite such prominence, the lifecycle evaluation of the NiSi-PS catalyst in the titled transformation was skipped.

Excluding Ni-based materials, another heterogeneous non-noble mono-metal catalyst, *i.e.*, copper impregnated on silica

Table 3 Physical–chemical properties of various TiO_2 and Ni/TiO_2 materials

Physical–chemical properties	P25	P90	UV100	PC500
	TiO_2support			
Composition of crystallized phase (%)	R: 21 A:79	R: 10 A:90	A: 100	A: 100
Average crystallite size (nm)[a]	R: 32 A:22	R: 23 A:13	9	7
BET surface area ($m^2\ g^{-1}$)	55	90	330	336
Pore volume ($cm^3\ g^{-1}$)	0.12	0.24	0.22	0.21
	Catalyst (10 wt% Ni/TiO_2)			
Size of crystallites (nm)[b]	12	15	8	8
Acidity (μmol m^{-2})[c]	1.7	1.8	0.5	0.4
H_2-TPR temp (°C)[d]	460	465	425	420
2,5-DMF yield (%)	24	54	79	85
2,5-DMTHF yield (%)	54	29	6	5

[a] Determined by XRD analysis for the (101) and (110) peaks of anatase (A) and rutile (R). [b] Determined by XRD analysis for the metallic nickel. [c] Determined by NH_3-TPD analysis. [d] Determined by H_2-TPR measurement; temperature at the maximum H_2 consumption rate.

(Cu/SiO_2), was also used for the generation of 2,5-DMTHF.[34] Three typical techniques including excessive impregnation (EI), disposition-precipitation (DP) and hydrothermal (HT) method were employed for the construction of $Cu@SiO_2$ materials at different pH values (6.5, 8.5 and 9). Upon treating 5-HMF with 6 bar H_2 over different Cu/SiO_2 catalysts at 200 °C in THF, the yield of 2,5-DMTHF was ranked in the sequence of 23 wt% Cu/SiO_2-DP-9 (0.5%) < 32 wt% Cu/SiO_2-EI (1.6%) < 31 wt% Cu/SiO_2-HT-8.5 (34.5%) < 33 wt% Cu/SiO_2-HT-6.5 (41.4%). These results might be because the Cu/SiO_2-HT samples encompassed a higher proportion of active Cu^0 species and smaller Cu particle size compared to other analogues.

Apart from non-precious metals, noble metallic catalysts have also been explored for the hydrodeoxygenation–hydrogenation cascade of 5-HMF. For instance, Chatterjee *et al.* screened a series of supported noble metal catalysts (M/SP; M = Pt, Pd, Rh and Ru; SP = AC, MCM-41 and Al_2O_3) for the transformation of 5-HMF in a H_2O-$scCO_2$ solvent system, wherein only 5 wt% Pd/C was capable of furnishing 2,5-DMTHF in a maximum yield of 80% under testing conditions (10 bar H_2, 100 bar CO_2, 130 °C, 2 h).[35] Otherwise, either 5-MFMAL or 2,5-DMF was dominantly accumulated when the reaction was tested with other supported catalysts. It is imperative to highlight that the CO_2 pressure and the reaction media had such a profound impact on the product distribution. More specifically, a high pressure of CO_2 (>100 bar) helped to enhance the selectivity of 2,5-DMTHF by triggering homogeneity between the gas phase (CO_2 + H_2) and the liquid phase (5-HMF + H_2O), whereas lowering the CO_2 pressure (<100 bar) accounted for the selectivity for 2,5-DMF and tetrahydro-5-methyl-2-furanmethanol (THMFM). In parallel, the replacement of H_2O-$scCO_2$ media with both monophasic (H_2O or CO_2) and biphasic systems (H_2O + organic solvents) led to the supression of 2,5-DMTHF production. The practicality of this catalytic protocol, besides 5-HMF, could be applied to FF to offer a quantitative yield of 2-MTHF after 2 h at 80 °C.

Alternatively, 95% conversion of 5-HMF along with 64% yield of 2,5-DMTHF was afforded when the Pd/C-mediated cascade reaction was executed in 1,4-dioxane with 3 bar H_2 at 120 °C and 15 h.[36] While several additives, such as formic acid, acetic acid, CO_2 or H_2O-CO_2 mixture, drastically reduced the selectivity for 2,5-DMTHF because the hydrogenation of the furan ring was suppressed, the introduction of 10 equiv. of dimethyl dicarbonate as a CO_2 alternative proved to be conducive to increasing the 2,5-DMTHF yield to over 95%. Unfortunately, a clear understanding of this phenomenon in this study has yet to be established.

In another study with Pd decorated on HBr-modified Al_2O_3 catalyst (5 wt% Pd/Al_2O_3-HBr), 61.9% selectivity for 2,5-DMTHF with 88.3% conversion of 5-HMF was observed in THF under mild conditions (20 bar H_2, 60 °C, 1 h).[37] Contrastingly, trials with other Pd-based catalysts—such as Pd/Al_2O_3, Pd/Al_2O_3-Br_2, Pd/Al_2O_3-NH_4Br, Pd/Al_2O_3-BrBen, Pd/Al_2O_3-ClBen, Pd/C, and Pd/SiO_2—for a similar transformation were unsuccessful, preferentially producing 2,5-DMF or 2,5-BHMTHF instead of 2,5-DMTHF. This can be accredited to the promotion of Br atoms, which not only created Brønsted acid sites proximal to metal sites but also generated new Pd–Br sites for the heterolytic dissociation of H_2.

Apart from Pd, other active noble metals (*i.e.*, Ru, Rh and Ir) were also adopted for the hydrodeoxygenation and/or hydrogenation reaction.[38] Typically, the treatment of 5-HMF with 50 bar H_2 and commercial 5 wt% Ru/C catalyst efficiently produced 2,5-DMTHF at yields of 74% (3 h) and 78% (16 h) in 1,4-dioxane and 180 °C.[39] More intriguingly, it was discovered that the switchable formation of 2,5-DMTHF and 2,5-DMF over Ru/C catalyst pertained to the quality of the commercial 5-HMF feedstock. Although commercial biomass-derived 5-HMF reagents were supplied in high purity (≥97%), the existence of DMSO as the main impurity significantly suppressed the formation of 2,5-DMTHF. More precisely, the higher the concentration of DMSO, the lower the yield of 2,5-DMTHF, even with a prolonged reaction time (Fig. 1a). These salient findings were substantiated by SEM-EDX, XPS, and CO chemisorption analyses of the recovered Ru/C catalyst, wherein sulfur species (*e.g.*, sulfates, sulfonates, disulfides or thiols) emanating from the thermal degradation of DMSO during the hydrotreatment of 5-HMF were found to strongly attach to the catalyst, dramatically modifying the Ru surface and/or blocking the Ru active sites for the hydrogenation. Last but not least, the presence of acids (*i.e.*, *p*-TsOH, HCl, and H_2SO_4) as potential impurities in the 5-HMF feedstock also posed a threat to the selectivity of 2,5-DMTHF, but their effects were far less pronounced than that of DMSO at equal concentrations (Fig. 1b).

Apart from Ru/C, other precious metals impregnated on carbon (M/C, M = Pd, Pt, Rh, and Ir) were also appraised for the title transformation.[40] Experimental results showed that the selectivity for 2,5-DMTHF at full 5-HMF conversion was ranked in the order of 5 wt% Rh/C (36%) < 1 wt% Ir/C (81.1%) < 5 wt% Ru/C (85.6%), whereas 2,5-BHMTHF (93%) and 2,5-DMF (85%) were principally produced over 5 wt% Pd/C and 5 wt% Pt/C, respectively, under the tested conditions (50 bar H_2, 180 °C, 16 h). Similar to Ru/C, the introduction of DMSO also resulted in a dramatic drop in the yield of 2,5-DMTHF for both Rh/C and Ir/C catalysts. Furthermore, the influence of different sulfur species (*i.e.*, dibutyl sulfide, 1-butanethiol, dimethyl sulfone, and methane sulfonic acid) as contaminants on the Ru/C-

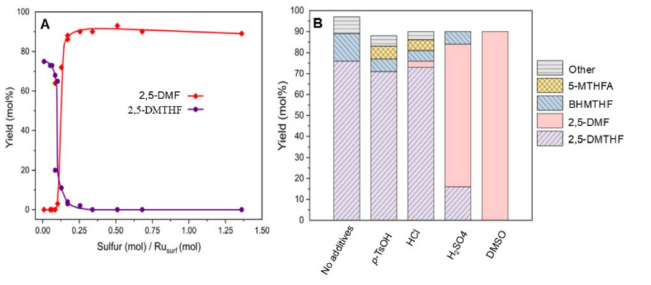

Fig. 1 The impact of: (a) DMSO-derived sulfur and (b) other potential contaminants in the 5-HMF feedstock on the yield of 2,5-DMTHF. Standard conditions: 5-HMF (3.96 mmol), 5 wt% Ru/C (100 mg), contaminant (20 μmol), 1,4-dioxane (40 mL), H_2 (50 bar), 180 °C, 4 h. Reproduced with permission from ref. 39 Copyright (2021) American Chemical Society.

mediated transformation of 5-HMF was also scrutinized. Interestingly, it was discovered that the introduction of all sulfur compounds at the same concentration resulted in a dramatic shift of selectivity from 2,5-DMTHF to 2,5-DMF, except for methane sulfonic acid. This observation was consistent with the XPS data of Ru/C catalysts recovered from the hydrotreatment of 5-HMF in the presence of dibutyl sulfide, 1-butanethiol and dimethyl sulfone. The catalyst deactivation was ascribed to the accumulation of *in situ* reduced sulfur species on the Ru surface.

In continuation of the monometallic study, the practicality of supported multi-metals towards 2,5-DMTHF production was also investigated. As described by Kong *et al.*, the switchable formation of 2,5-DMF and 2,5-DMTHF over a collection of hydrotalcite-derived Ni–Al catalysts (Ni/Al molarity ~2.90) was readily accomplished by regulating the catalyst properties and reaction time.[33] Particularly, empirical data from H_2, NH_3, and CO TPD analyses indicated that the modulation of the calcination temperature (*i.e.*, 300, 450, 600, 750 and 850 °C) used to prepare the Ni–Al samples led to substantial changes in the catalyst properties (*i.e.*, surface Lewis acidity, concentration of Ni^0 species, and strength of NiO-Al_2O_3 interaction), where the high-temperature treatment resulted in a large amount of acid sites but a low density of metallic Ni sites (Fig. 2a). As a result, only Ni–Al-750 and Ni–Al-850 exhibited outstanding catalytic performance, achieving excellent productivity of both 2,5-DMF and 2,5-DMTHF within an appropriate time at 180 °C in 1,4-dioxane (Fig. 2b). Despite its remarkable resistance to Ni sintering, the recovered Ni–Al-850 suffered significant deactivation due to the gradual deposition of carbonaceous materials on the active sites over multiple cycles.

Another example is the exploitation of Cu–Zn nanoalloy, where a mixture of 2,5-DMF (72.7%) + 2,5-DMTHF (24.3%) was produced from a 10% solution of 5-HMF in cyclopentyl methyl ether (CPME) at 220 °C for 6 h.[41] Operating the same reaction under milder conditions (200 °C and 3 h) gave minute changes in the aggregate yield (~96%) but significantly increased the yield of 2,5-DMF up to 90%. Moreover, it is noticed that the selectivity of 2,5-DMTHF was reduced upon replacing CPME with other organic solvents (*i.e.*, ethanol, 2-propanol, 2-MTHF, and methyl isobutyl carbanol), even at a high temperature of 220 °C and an elongated reaction time of 18 h. Moreover, substantial increases in the ratio of 2,5-DMF to 2,5-DMTHF were witnessed due to the significant accumulation of organic species on the surface of the spent Cu–Zn nanoalloy after multiple recycling tests.

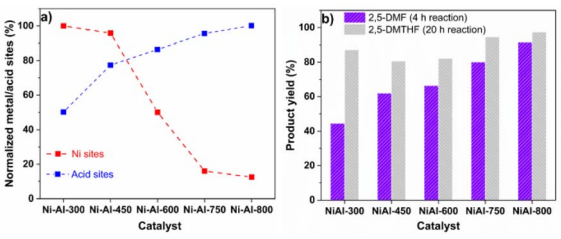

Fig. 2 (a) Properties of Ni–Al catalysts calcined at different temperatures. (b) Switchable delivery of 2,5-DMF and 2,5-DMTHF from 5-HMF over various Ni–Al catalysts with regulated reaction time.

At a low temperature of 90 °C in THF, Gupta *et al.* reported that 5-HMF was quantitatively converted into 2,5-DMTHF in 32% yield with the participation of Cu–Ni alloy decorated on hydrotalcite (Cu–Ni/HT; 18.7 wt% Cu, 5.7 wt% Ni, HT with a Mg/Al molar ratio of 3.0).[42] Meanwhile, 53% selectivity for 2,5-DMTHF was acquired over palladium-tungstate carbide supported on activated carbon (5 wt% Pd–30 wt% W_2C/AC) when the conversion of 5-HMF was fully accomplished after 3 h of reaction at 180 °C in THF.[43] By comparison with 5 wt% Pd–30 wt% W_2C/AC, an assortment of benchmark carbon-supported catalysts including Ni–W_2C/AC, Cu–W_2C/AC and Cu–Ru/AC, predominantly produced 2,5-DMF or 5-MFF.

Starting with various lab-made LDH-structured Cu-based catalysts, such as 16.8 wt% Cu/$MgAlO_x$, Co–Cu/3$CoAlO_x$ (11.1 wt% Cu, 33.5 wt% Co) and Co–Cu/5$CoAlO_x$ (8.6 wt% Cu, 41.7 wt% Co), Zhang and colleagues discovered that the Co–Cu/5$CoAlO_x$ reduced from corresponding $CuCo_5Al_2$-LDH precursor was solely qualified for both C–O hydrogenolysis and furan ring hydrogenation of 5-HMF to achieve 2,5-DMTHF in 83.6% yield and 100% selectivity after a 20-hours reaction in 1,4-dioxane at 180 °C.[44] On the contrary, 2,5-BHMF (92.7%) and 2,5-DMF (98.5%) were preferentially yielded under the catalysis of Cu/$MgAlO_x$ and Co–Cu/3$CoAlO_x$, respectively, when the reaction time was shortened to 5 h. Notwithstanding their similar structure of matrix-encapsulated Cu NPs, the stark disparity between the Cu/$MgAlO_x$ and Co–Cu/$CoAlO_x$ series towards the product distribution can be attributed to the presence of defective cobalt oxide (CoO_x with enriched oxygen vacancies) and metallic Co–Cu interfaces. More specifically, interfacial metal-oxide sites (Cu–O–Co–V_O) and a high number of metallic Co–Cu interfaces in Co–Cu/5$CoAlO_x$ concertedly facilitated sequential reactions to smoothly convert 5-HMF into 2,5-DMTHF as compared to both Cu/$MgAlO_x$ and Co–Cu/3$CoAlO_x$.

To convert 5-HMF into 2,5-DMTHF at ambient temperature, the catalysis of AC-supported Pd–Cu nanoalloys endowed with two specific engineered crystallographic phases, *i.e.*, face-centred cubic (FCC) and body-centred cubic (BCC) structure, was probed by Li and coworkers.[45] A 2,5-DMF yield of 93.6% was achieved with the assistance of Pd–Cu/AC-BCC, whereas a complex mixture of 2,5-DMF (9.3%) + 2,5-DMTHF (24%) + 2,5-BHMTHF (41.5%) was concomitantly produced under the same conditions (40 bar H_2, 30 °C, 20 h) over Pd–Cu/AC-FFC. Supported by a set of control experiments and DFT calculations, the arrangement of surface atoms as well as different adsorption modes of furanic intermediates on FCC (100) and BCC (111) metal surface were identified as the reason for that stark disparity.

In summary, there are crucial issues pertaining to the application of active catalysts and/or reaction parameters for the successful one-pot transformation of 5-HMF to 2,5-DMTHF. As compared to BHMTHF and 2,5-DMF synthesis, higher temperatures and longer times are typically employed. Regarding the catalyst, heterogeneous bifunctional metal catalysts containing both metallic and acidic active sites are deemed to be of great convenience. As such, the importance of the active

phase, the dispersion of metal species, and the well-tuned acidity of support are important factors governing the hydrogenation of C=O and hydrogenative cleavage of C–OH, and the reduction of the C=C bond, wherein 2,5-DMF is regarded as the principal intermediate. On top of that, the imbalance and insufficient contact between metal and acid sites would limit the hydrodeoxygenation efficiency of 5-HMF towards 2,5-DMTHF.

3. Catalytic hydrodeoxygenation-transfer hydrogenation cascade of FF and 5-HMF

In addition to the conventional hydrodeoxygenation–hydrogenation pathway using H_2, the valorisation of biomass-derived FF and 5-HMF can be accomplished through the catalytic hydrodeoxygenation-transfer hydrogenation route.[46,47] In this alternative strategy, cheap and available alcohols (*e.g.*, methanol, ethanol, 2-propanol, 2-butanol, and cyclohexanol) or formic acid are generally employed as both hydrogen donor and solvent, addressing several critical problems (*i.e.*, safety, storage, and transportation) as witnessed in the H_2-driven route. Therefore, this section will focus on the practicality of hydrogen alternatives and the performance of different supported mono-/multi-metallic catalysts in the hydrodeoxygenation-transfer hydrogenation cascade.

3.1. Preparation of 2-MTHF from FF

The first trial of the tandem hydrodeoxygenation-transfer hydrogenation of FF towards 2-MTHF was carried out by Chang *et al.*, in which a collection of heterogeneous metallic catalysts (M/SP; M = Cu, Pd, Cu–Ni, Cu–Ru and Cu–Pd; SP = ZrO_2, Al_2O_3, SiO_2, and TiO_2) with 2-propanol were employed.[48] Of these, 10 wt% Cu–5 wt% Pd/ZrO_2 with an ideal Cu/Pd ratio displayed the highest catalytic efficiency, selectively yielding 2-MTHF in 78.8% after reacting for 4 hours at 220 °C. This result originated from: (i) the critical role of acid–base sites on ZrO_2 in facilitating the absorption and dissociation of H atom from 2-propanol; and (ii) the interplay between Cu and Pd metal. Based on the product evolution coupled with control experiments on potential intermediates (*i.e.*, THFA, 2-MF, 2-IPOMF, and GVL) established during the conversion of FF, the assembly of 2-MTHF over 10 wt% Cu–5 wt% Pd/ZrO_2 catalyst is suggested to follow the major pathway shown in Scheme 4.

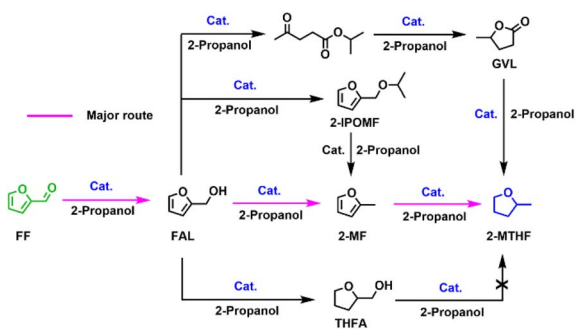

Scheme 4 Reaction pathway leading to 2-MTHF from the catalytic hydrodeoxygenation-transfer hydrogenation of FF in 2-propanol.

By the same token, 100% conversion of FF and 51% selectivity for 2-MTHF were achieved at 250 °C using an Al_2O_3-supported bimetallic Cu–Ni catalyst (20 wt% Cu–40 wt% Ni/Al_2O_3) with 2-propanol.[49] In another experiment involving 5 wt% Pd/Al_2O_3 as the catalyst and formic acid as a terminal reductant, 2-MTHF was directly produced from FF with a selectivity of 59% after 18 hours of reaction at 210 °C.[50]

3.2. Preparation of 2,5-DMTHF from 5-HMF

Following the same strategy for 5-HMF, a nitrogen-doped carbon-decorated copper catalyst (NC-Cu/MgAlO, 31.6 wt% Cu) was designed to produce 2,5-DMTHF.[51] Extensive characterization analyses revealed that this well-defined catalyst encompassed several distinct characteristics of: (i) large amount of strong and super strong basic sites on the surface; (ii) strong metal–support interaction (*e.g.*, Cu^+–O–Mg/Al or Cu^+–NC mode); (iii) high dispersion with small particle size of Cu NPs; and (iv) high $Cu^+/(Cu^0 + Cu^+)$ molar ratio as compared to both Cu/MgAlO and NC-Cu/Al_2O_3. Indeed, these prominent features were key factors governing the reactivity and robustness of high-performance NC-Cu/MgAlO throughout the hydrodeoxygenation-transfer hydrogenation of 5-HMF. Consequently, a 94.6% yield of 2,5-DMTHF was acquired when the reaction was executed in cyclohexanol at 220 °C for 3.3 h. On top of that, the original activity of the spent NC-Cu/MgAlO catalyst was well-preserved after five successive runs without any requirement for regeneration.

4. Continuous-flow hydrodeoxygenation–hydrogenation cascade of FF and 5-HMF

Considering the merits of flow chemistry during the valorisation of biomass platform molecules into valuable fuels and chemicals, several research groups have applied this convenient process to produce 2-MTHF and 2,5-DMTHF (Table 4).[52,53] As an example, Stevens and colleagues successfully designed a continuous-flow apparatus equipped with two separate reactors to produce 2-MTHF in the presence of H_2 and $scCO_2$.[54] As illustrated in the tandem reactor setup (Fig. 3a), an 82% yield of 2-MTHF was obtained when the reaction mixture was flowed downward from the top, passing successively through catalyst beds of commercial $Cu_2Cr_2O_x$ (240 °C) and 5 wt% Pd/C (300 °C). According to the authors, the beneficial employment of $scCO_2$ medium in this protocol not only reduced the mass-transfer limitations but also increased the solubility of FF. Moreover, the prominence of this continuous process was acknowledged by the fact that divergent products could be achieved in high selectivity by simple regulation of the temperature and/or H_2 concentration in each reactor (Fig. 3b). Unfortunately, the reusability of these catalyst bed systems was not reported in this study.

Table 4 Direct production of 2-MTHF and 2,5-DMTHF by continuous-flow process

Catalyst	Reaction conditions	Conv. (%)	Yield (%)	Ref.
$Cu_2Cr_2O_x$ + 5 wt% Pd/C	FF (0.05 mL min^{-1}), $scCO_2$ (1 mL min^{-1}), H_2 (15 MPa) Reactor I: $Cu_2Cr_2O_x$ (1900 mg), 240 °C Reactor II: 5 wt% Pd/C (500 mg), 300 °C	100	82	54
$Cu_2Cr_2O_x$ + 5 wt% Pd/C	FF (5 mL h^{-1}), H_2 (15 l h^{-1}), 175 °C $Cu_2Cr_2O_x$-TL (30×10^3 mg), 5 wt% Pd/C-BL (21×10^3 mg), 175 °C	100	91	55
	FF (5 mL h^{-1}), H_2 (15 l h^{-1}), 200 °C $Cu_2Cr_2O_x$-TL (30×10^3 mg), 5 wt% Pd/C-BL (21×10^3 mg)	100	91	
	FF (5 mL h^{-1}), $Cu_2Cr_2O_x$-TL (30×10^3 mg), 5 wt% Pd/C-BL (21×10^3 mg), H_2 (15 l h^{-1}), 225 °C	100	86	
	FF (5 mL h^{-1}), $Cu_2Cr_2O_x$-TL (30×10^3 mg), 5 wt% Pd/C-BL (21×10^3 mg), H_2 (15 l h^{-1}), 250 °C	100	82	
$Cu_2Si_2O_5(OH)_2$ + 5 wt% Pd/SiO_2	$Cu_2Si_2O_5(OH)_2$-TL (2500 mg), 5 wt% Pd/SiO_2-BL (500 mg), 180 °C, WHSV = 0.19 h^{-1}	99.1	68.6	56
	$Cu_2Si_2O_5(OH)_2$-TL (1500 mg), 5 wt% Pd/SiO_2-BL (1500 mg), 180 °C, WHSV = 0.19 h^{-1}	98.4	93.3	
	$Cu_2Si_2O_5(OH)_2$-TL (1000 mg), 5 wt% Pd/SiO_2-BL (2000 mg), 180 °C, WHSV = 0.19 h^{-1}	100	97.1	
	$Cu_2Si_2O_5(OH)_2$-TL (500 mg), 5 wt% Pd/SiO_2-BL (2500 mg), 180 °C, WHSV = 0.19 h^{-1}	100	76.1	
8.5 wt% Co/Al_2O_3 + 8.2 wt% Ni/SiO_2	FF (0.03 mL min^{-1}), 8.5 wt% Co/Al_2O_3-TL (2500 mg), 8.2 wt% Ni/SiO_2-BL (2000 mg), H_2 (10 bar), 180 °C, WHSV = 0.46 h^{-1}	100	83.6	57
8.5 wt% Co/Al_2O_3 + 7.4 wt% Ni/Al_2O_3	FF (0.03 mL min^{-1}), 8.5 wt% Co/Al_2O_3-TL (2100 mg), 7.4 wt% Ni/Al_2O_3-BL (1500 mg), H_2 (10 bar), 180 °C, WHSV = 0.46 h^{-1}	100	78	
8.5 wt% Co/Al_2O_3 + 7.4 wt% Ni/Al_2O_3	FF (0.03 mL min^{-1}), 8.5 wt% Co/Al_2O_3-TL (2500 mg), 7.4 wt% Ni/Al_2O_3-BL (2000 mg), H_2 (10 bar), 180 °C, WHSV = 0.46 h^{-1}	100	87.3	
10 wt% Pt/C	FF (3 mL h^{-1}), H_2 (12 mL min^{-1}), 180 °C	100	46.7	58
10 wt% Ni/C		100	52.9	
6.5 wt% W–12.2 wt% Cu/γ-Al_2O_3	FF (3 mL h^{-1}), H_2 (30 bar), 220 °C, WHSV = 0.5 h^{-1}	100	33	59
10 wt% Pd/C	5-HMF (8 mmol),1-propanol (100 mL), H_2 (33 bar), 180 °C	100	55	60
30 wt% Ni–15 wt% Cu/ZrO_2	5-HMF (1.5% in 1-butanol), H_2 (15 bar), 275 °C, 7 h, WHSV = 0.15 h^{-1}	100	60	61
15 wt% Ni–15 wt% Cu/K-C	5-HMF (1.5% in 1-butanol), cat. (500 mg), H_2 (15 bar), 275 °C, 7 h, WHSV = 0.15 h^{-1}	100	41.9	62
15 wt% Ni/K-C		100	43.8	
15 wt% Ni–15 wt% Cu/K-TC		100	44.5	

To avoid the complicated setup of multiple reactors, Wabnitz *et al.* performed the hydrodeoxygenation–hydrogenation cascade of FF in a single tubular reactor packed with a two-stage catalyst bed comprising $Cu_2Cr_2O_x$-TL (TL denoted as top layer) + 5 wt% Pd/C-BL (BL denoted as bottom layer).[55] Attractively, the simple continuous operation under a H_2 flow produced 2-MTHF in good to excellent yields at different temperatures (175–250 °C). Similarly, the fixed-bed reactor assembled with a double catalyst bed composed of $Cu_2Si_2O_5(OH)_2$-TL + Pd/SiO_2-BL gave an excellent yield of 2-MTHF at 180 °C under atmospheric H_2 pressure.[56] As represented in Fig. 4, both the ideal mass packing ratio of $Cu_2Si_2O_5(OH)_2$ over Pd/SiO_2 and their proper arrangement in the thermostat segment of the reactor were indispensable to guaranteeing the success of this approach. In other words, insufficiency of either Pd or Cu active species resulted in low productivity of 2-MTHF. Once again, no valuable information on the lifecycle of the catalyst beds was provided for the aforementioned approaches.

Recently, a fixed-bed tubular reactor furnished with a two-stage non-precious metallic catalyst system comprising either 8.5 wt% Co/Al_2O_3-TL + 8.2 wt% Ni/SiO_2-BL or 8.5 wt% Co/Al_2O_3-TL + 7.4 wt% Ni/Al_2O_3-BL was developed for the continuous production of 2-MTHF.[57] In both cases, satisfactory yields of 2-MTHF (>70%) were acquired at 180 °C under 10 bar H_2 pressure, and slightly declined after 8 h of time on stream. This occurrence can be expounded by the deactivation of metal catalysts, which is stemmed from the deposition of carbonaceous materials on the active sites throughout the FF transformation. Especially, trials on separate control reactions showed that the efficacy of FF hydrodeoxygenation towards 2-MF assisted by supported cobalt catalysts was strongly influenced by the Lewis acidity of carriers (Fig. 5a), while the

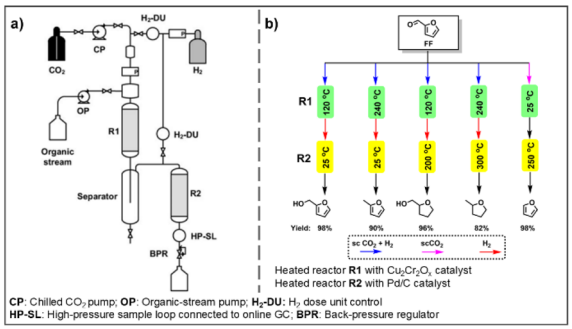

Fig. 3 (a) Automated continuous-flow apparatus diagram. (b) Product distribution with simple modulation of temperature and/or H_2 pressure.

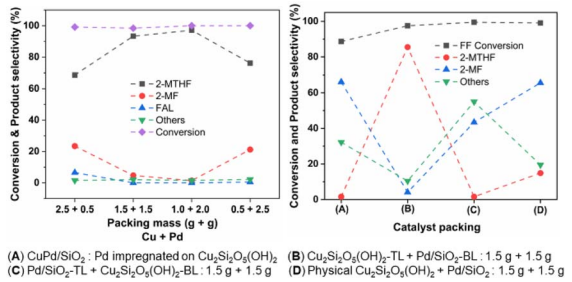

Fig. 4 Influence of mass packing and packing method of catalyst bed on the continuous production of 2-MTHF in a single fixed-bed reactor.

hydrogenation of 2-MF only worked well with Ni-based catalysts (Fig. 5b).

In another study conducted by Wang *et al.*, the production of 2-MTHF from FF was achieved in a tubular-flow reactor endowed with a single bed of carbon-supported metal catalysts (10 wt% M/C; M = Ni, Co, Pt, Ni–Fe, and Pt–Co_3).[58] It was found that 2-MTHF was selectively produced at yields of 46.7% and 52.9% under the catalysis of 10 wt% Pt/C and 10 wt% Ni/C, respectively, when the reaction was conducted at 180 °C and 33 bar H_2. Subsequently, the deployment of Cu/γ-Al_2O_3 modified with WO_x promoter (W–Cu/γ-Al_2O_3; 6.5 wt% W and 12.2 wt% Cu) for the assembly of 2-MTHF was presented by Kalong and coworkers.[59] Exhaustive characterization of the structure and morphology disclosed that the doping of WO_x species into Cu/γ-Al_2O_3 resulted in the enhancement of both metal–support interactions and the number of acidic sites,

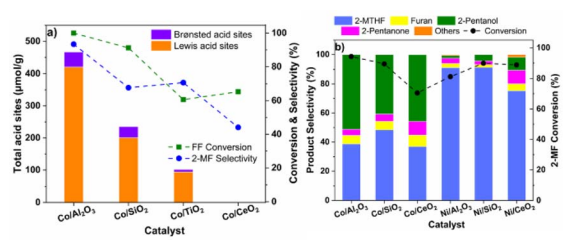

Fig. 5 The effect of catalysts on: (a) the hydrodeoxygenation of FF into 2-MF; and (b) the hydrogenation of 2-MF into 2-MTHF.

beneficially boosting the reactivity of the reduced W–Cu/γ-Al_2O_3 catalyst. Accordingly, the highest 2-MTHF yield of 33% was achieved when the reaction was conducted under harsh conditions of 220 °C and 30 bar H_2. Regarding the durability, the accumulation of carbon or intermediates on the catalyst surface was the primary reason for the deactivation of W–Cu/γ-Al_2O_3 over time.

With 5-HMF as the substrate, the continuous flow synthesis was carried out in a tubular reactor packed with a catalyst bed of 10 wt% Pd/C, yielding 2,5-DMTHF at 55% at 180 °C and 33 bar H_2 in 1-propanol.[60] Following this work, Viar *et al.* implemented the hydrodeoxygenation–hydrogenation cascade of 5-HMF in a fixed-bed reactor in the presence of ZrO_2-supported bimetallic Ni–Cu catalysts.[61] For that purpose, bimetallic catalysts with various amounts of Ni and Cu species were prepared by either co-impregnation (xNiyCu/ZrO_2) or stepwise impregnation (xNi–yCu/ZrO_2, Cu was first impregnated; yCu–xNi/ZrO_2, Ni was first impregnated), where the amount of Ni loading coupled with the order of metal impregnation during the catalyst preparation were major determinants of how 2,5-DMTHF was selectively produced from 5-HMF. Among all catalysts, reduced 30 wt% Ni–15 wt% Cu/ZrO_2 exhibited the best reactivity, producing a mixture of 2,5-DMF (28.8%) + 2,5-DMTHF (60%) after 7 h of time on stream under specific conditions (15 bar H_2, 275 °C, WHSV = 0.15 h^{-1}). Unfortunately, a long period of time on stream (>7 h) appeared to substantially hinder the formation of 2,5-DMTHF due to the progressive oxidation of Ni^0 species in 30 wt% Ni-15 wt% Cu/ZrO_2 throughout the transformation. Later, single metals (Ni or Cu) and bimetals (Ni–Cu, Cu was first impregnated) decorated on kaolin-incorporated untreated carbon (K-UC) and treated carbon (K-TC) were also examined for the titled process.[62] The reaction profile indicated that only 15 wt% Ni/K-UC, 15 wt% Ni–15 wt% Cu/K-UC and 15 wt% Ni–15 wt% Cu/K-TC exhibited high selectivity towards 2,5-DMTHF, in which the yield of the target product was arranged in the order of 15 wt% Ni–15 wt% Cu/K-UC (41.9%) < 15 wt% Ni/K-UC (43.8%) < 15 wt% Ni–15 wt% Cu/K-TC (44.5%) after 4 h of time on stream under the specified operating conditions (15 bar H_2, 275 °C, WHSV = 0.15 h^{-1}). However, it was observed that the formation of 2,5-DMTHF diminished over time (>4 h) and was almost suppressed by the end of the process (25 h) in all cases, likely due to the carbon buildup on the catalyst surface.

5. One-pot valorisation of biomass materials into 2-MTHF and 2,5-DMTHF

Apart from FF and 5-HMF feedstocks, the production of 2-MTHF and 2,5-DMTHF can be accomplished through the cascade transformation (hydrolysis–dehydration–hydrodeoxygenation–hydrogenation) of carbohydrates or raw lignocellulose (Table 5). For example, 2-MTHF (80%) and 2,5-DMTHF (54–82%) were produced from xylose and other sugars (glucose, inulin, sucrose and cellulose), respectively, using a homogeneous catalyst system ($RhCl_3 \cdot xH_2O$ + HI) and a biphasic solvent of H_2O + chlorobenzene.[63,64] By the same token, yields for 2,5-DMTHF of 41% and 2-MTHF of 46.2% were attained from crude

Table 5 Reductive transformation of fructose into 2,5-DMTHF

Catalyst system	Reaction conditions	Conv. (%)	Yield (%)	Ref.
5 wt% Ru/C + [Bmim]Cl	Step I: Fructose (360 mg), [Bmim]Cl (1000 mg), 0.5 h Step II: 5 wt% Ru/C (100 mg), THF (25 mL), H_2 (50 bar), 250 °C, 5 h	— —	78[a] 31.3	66
Pt/C-S (5 wt% Pt, 1.57 wt% S)	Fructose (4954 mg), 5 wt% Pt/C-S (500 mg), 95% EtOH solution (50 mL), H_2 (103 bar), 175 °C, 2 h	—	47	67
4.6 wt% Pd/AC + H_2SO_4 + NaCl	Fructose (100 mg), 4.6 wt% Pd/AC (20 mg), 0.25 M H_2SO_4 + 0.25 g mL^{-1} NaCl (1 mL), Et_2O (9 mL), H_2 (4 bar), 130 °C, 12 h	100	69.7	68

[a] 5-HMF.

corn stover and pretreated rice straw, respectively, under the catalysis of $RhCl_3$ + HCl + NaI in a biphasic solvent of water + toluene.[64,65] However, it is imperative to note that these homogeneous protocols are achieved at the great expense of high-cost Rh catalysts, corrosive nature of mineral acids, and toxic organic solvents (chlorobenzene or toluene).

In 2015, Li and colleagues described the successful one-pot valorisation of fructose into 2,5-DMTHF leveraging a Ru/C catalyst and green solvent system (BMimCl + THF).[66] According to the reported protocol, 5-HMF was initially yielded at 78% upon treating fructose with BMimCl at 130 °C for 0.5 h, which was subsequently converted into 2,5-DMTHF (31.3%) with the introduction of 5 wt% Ru/C, THF and 50 bar H_2 at specific conditions (250 °C, 5 h). The key function of the BMimCl + THF system in this approach was rationalized by the fact that BMimCl not only catalysed the fructose-to-5-HMF dehydration but also enhanced the Ru/C-mediated hydrodeoxygenation of 5-HMF by altering the electronic density of Ru species. Furthermore, THF serving as a co-solvent also helped to suppress the ring opening and other side reactions. The production of byproducts from the Ru/C-catalysed hydrotreatment of fructose-derived 5-HMF in THF without the introduction of BMimCl is mechanistically proposed in Scheme 5.

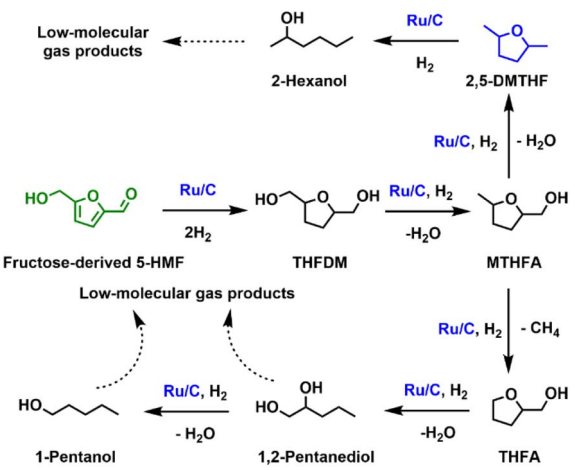

Scheme 5 Tentative mechanism for the establishment of byproducts during the hydrodeoxygenation–hydrogenation of fructose-derived 5-HMF over Ru/C catalyst.

Concurrently, Jackson and coworkers employed commercial sulfided platinum on carbon (5 wt% Pt/C-S, 1.57 wt% S) to produce 2,5-DMTHF from fructose.[67] After reacting for 2 hours at 175 °C with 103 bar H_2 in 95% EtOH solution, this catalyst afforded 2,5-DMTHF in 47% yield with a *cis*/*trans* ratio of 2.45. Herein, it should be highlighted that the content of both the reaction media and the sulfur contaminant significantly impacted the reaction outcome. Specifically, either decreasing the concentration of EtOH or replacing EtOH by H_2O drastically reduced the selectivity of 2,5-DMTHF due to the rapid decomposition of fructose in such conditions. Additionally, the recovered Pt/C-S catalyst, after several recycles, showed substantial depletion of sulfur species relative to the pristine sample, thus leading to a preference for sugar alcohols (mannitol + sorbitol) rather than 2,5-DMTHF. Based on product distribution and computational calculations, an alternative mechanism for the direct manufacture of 2,5-DMTHF from fructose is proposed in Scheme 6. At the initial stage, 2,5-hexandione intermediate is preferably triggered through the dehydration-ring opening cascade of fructose, which subsequently undergoes a sequence of hydrogenation and cyclization to generate a mixture of *cis* 2,5-DMTHF (71%) and *trans* 2,5-DMTHF (29%).

In another study presented by Li and coworkers, the co-catalysis of 4.6 wt% Pd/AC and H_2SO_4 enabled 69.7% selectivity towards 2,5-DMTHF (*cis*/*trans* ratio = 3.4) under mild conditions (4 bar H_2, 130 °C, 12 h) in a biphasic system of H_2O + Et_2O.[68] Contrarily, trials with other Brønsted acids (HCl and Amberlyst 15) or different reaction media (H_2O, Et_2O, H_2O + cyclohexane, H_2O + hexane, and H_2O + THF) appeared to diminish the selectivity for 2,5-DMTHF to a great extent. Especially, the introduction of DMSO into the H_2O + Et_2O system also entirely diverted the reaction pathway, resulting in undesired final products (2,5-DMF + 2,5-HDO or 5-HMF + 5-MFF) *in*

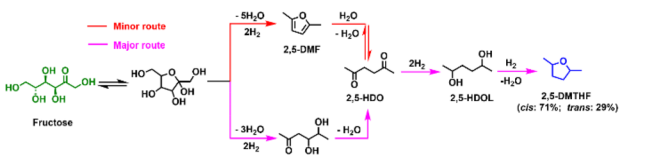

Scheme 6 Suggested mechanism for the reductive valorisation of fructose into 2,5-DMTHF.

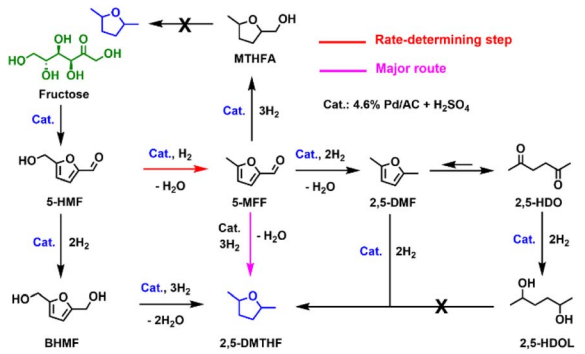

Scheme 7 Suggested mechanism for the one-pot conversion of fructose into 2,5-DMTHF.

lieu of 2,5-DMTHF. In such circumstances, DMSO was shown to either facilitate the formation of carbonyl-containing byproducts or impair the hydrogenation capability of Pd/AC. Significantly overwhelmed by leaching and sintering of Pd NPs, the recovered Pd/AC was confronted with reactivity deterioration shortly after two consecutive runs. Supported by the outcome and percentage of *cis*-2,5-DMTHF originating from the control reaction of potential intermediates (*i.e.*, BHMF, 5-MFF, MTHFA, 2,5-DMF, 2,5-HDO, and 2,5-HDOL), the conversion of fructose-derived 5-HMF into 5-MFF is regarded as the rate-determining step and 2,5-DMTHF is majorly constituted from 5-MFF intermediate, as shown in Scheme 7.

6. Conclusion and outlook

Both FF and 5-HMF play key roles in modern biorefineries by supporting the transition from conventional fossil fuels to renewable biomass resources. In this article, state-of-the-art advancements on the catalytic transformation of FF, 5-HMF, carbohydrates, and lignocellulose into valuable 2-MTHF and 2,5-DMTHF with green reductants (H_2 and alcohols) were highlighted. For that purpose, an assortment of heterogeneous metallic catalysts with specific properties for the two-stage (hydrodeoxygenation–hydrogenation and hydrodeoxygenation-transfer hydrogenation) or cascade reactions (hydrolysis–dehydration–hydrodeoxygenation–hydrogenation) under batchwise or continuous-flow mode were summarized. Specifically, several parameters, such as structure–reactivity correlation, reaction variables, reusability, process design, and reaction pathway, were discussed in detail. Despite such considerable strides, several hurdles need to be addressed in future research to satisfy the demand for mass production and commercial application of bio-based 2-MTHF and 2,5-DMTHF:

(i) First, the presence of impurities (*i.e.*, inorganic elements, heavy metals, water, and acids) during the manufacture of FF and 5-HMF from raw biomass is a great concern, which negatively impacts the storage, conversion efficiency, and catalyst performance. Consequently, the purification by different techniques including distillation, solvent extraction, adsorption, and recrystallization is highly required for both FF and 5-HMF.

(ii) Second, improvements to catalyst design, including the use of non-precious metals, tunable supports, facile preparation methods, ease of recovery, strong resistance to water/deactivation (carbon deposition, sintering, leaching), and good regenerability, are essential for achieving low-cost and long-term operation.

Although the straightforward assembly of 2,5-DMTHF from fructose can bypass the refinement and purification of the 5-HMF intermediate, the yield of the target product is lower than expected. Therefore, multifunctional catalysts for such complicated transformations require precise fabrication with respect to tuneable composition, structure, distribution of active sites, and acid–base balance.

(iii) Third, mild operating conditions alongside the replacement of toxic organic solvents (*i.e.*, 1,4-dioxane, DMSO, and THF) with benign reaction media for the hydrodeoxygenation–hydrogenation cascade should be considered from the viewpoint of green and sustainable chemistry.

(iv) Lastly, several issues with the product separation, techno-economic and lifecycle assessment for the mass production of 2-MTHF and 2,5-DMTHF need to be thoroughly investigated.

In summary, innovative collaborations in multidisciplinary domains of catalyst/process design, reaction engineering, upstream-downstream integration, environmental protection, and policy-making are essential to ensure the commercialization of bio-based 2-MTHF and 2,5-DMTHF. We hope that this comprehensive review will promote the interest of both the academic and industrial communities in the valorisation of cheap and available biomass materials for a circular economy.

Data availability

No primary research results, software or codes have been included and no new data were generated or analyzed as part of this review.

Author contributions

Ngan Nguyen Le: data curation and writing the original draft; Ngan Tuan Nguyen: data curation and review; Hoang Long Ngo: formal analysis and review; Thanh Tung Nguyen: formal analysis, review, and editing; Cong Chien Truong: visualization, conceptualization, review, and writing the original draft.

Conflicts of interest

The authors declare that they have no competing financial interests or personal relationships that could have appeared to influence the work reported in this paper.

References

1 T.-Z. Ang, M. Salem, M. Kamarol, H. S. Das, M. A. Nazari and N. Prabaharan, *Energy Strat. Rev.*, 2022, **43**, 100939.
2 H. Stančin, H. Mikulčić, X. Wang and N. Duić, *Energy Rev.*, 2020, **128**, 109927.
3 P. Gallezot, *Chem. Soc. Rev.*, 2012, **41**, 1538–1558.

4 K. Alper, K. Tekin, S. Karagöz and A. J. Ragauskas, *Sustainable Energy Fuels*, 2020, **4**, 4390–4414.
5 R. Mariscal, P. Maireles-Torres, M. Ojeda, I. Sádaba and M. López Granados, *Energy Environ. Sci.*, 2016, **9**, 1144–1189.
6 A. A. Rosatella, S. P. Simeonov, R. F. M. Frade and C. A. M. Afonso, *Green Chem.*, 2011, **13**, 754–793.
7 G. W. Huber, S. Iborra and A. Corma, *Chem. Rev.*, 2006, **106**, 4044–4098.
8 M. D. Jackson and C. B. Moyer, in *Kirk-Othmer Encyclopedia of Chemical Technology*, 2010.
9 U. Addepally and C. Thulluri, *Fuel*, 2015, **159**, 935–942.
10 A. Sahu, C. Wang, C. Jiang, H. Xu, X. Ma, C. Xu and X. Bao, *Fuel*, 2019, **255**, 115659.
11 A. R. Alcantara and P. D. de Maria, *Curr. Green Chem.*, 2018, **5**, 86–103.
12 V. Pace, P. Hoyos, L. Castoldi, P. Dominguez de Maria and A. R. Alcantara, *ChemSusChem*, 2012, **5**, 1369–1379.
13 C. Zhang, Y. Wang, W. Yang and J. Zheng, *Org. Process Res. Dev.*, 2022, **26**, 2685–2693.
14 A. Iino, A. Cho, A. Takagaki, R. Kikuchi and S. Ted Oyama, *J. Catal.*, 2014, **311**, 17–27.
15 H. Althikrallah, E. F. Kozhevnikova and I. V. Kozhevnikov, *RSC Adv.*, 2022, **12**, 2287–2291.
16 D. Sharma, P. Choudhary, S. Kumar and V. Krishnan, *Small*, 2023, **19**, e2207053.
17 T. Mitsudome, *Catalysts*, 2024, **14**, 193.
18 F. Li, S. Jiang, T. Zhu, Y. Wang, T. Huang and C. Li, *ChemistrySelect*, 2020, **5**, 2271–2278.
19 S. Han, R. Gao, M.-S. Sun, Y. Zhou, W.-T. Chen, X. Liu, J. Qin, D. J. Tao and Z. Zhang, *J. Phys. Chem. C*, 2023, **127**, 14185–14196.
20 N. S. Date, N. S. Biradar, R. C. Chikate and C. V. Rode, *ChemistrySelect*, 2017, **2**, 24–32.
21 J. Lu, Y. Liu, J. Wang, Z. Zeng, L. Chen, S. Deng, J.-J. Zou and Q. Deng, *Appl. Catal., B*, 2024, **344**, 123622.
22 N. S. Date, A. M. Hengne, K. W. Huang, R. C. Chikate and C. V. Rode, *ChemistrySelect*, 2020, **5**, 9590–9600.
23 L. Huang, L. Wang, Z. Zhang, X. Guo, X. Zhang, J. M. Chabu, P. Liu and F. Tang, *J. Energy Chem.*, 2022, **71**, 225–233.
24 B. Yang, P. Chen, T. Zhu, G. Dong, H. Wang, Y. Liao, X. Zhang and L. Ma, *Energy Fuels*, 2024, **38**, 5303–5313.
25 Y. Peng, Z. Xu, L. Yu, X. Li and W. Yang, *Chem. Eng. J.*, 2023, **454**, 139746.
26 Y. Yang, Z. Du, Y. Huang, F. Lu, F. Wang, J. Gao and J. Xu, *Green Chem.*, 2013, **15**, 1932–1940.
27 S. Liu, Y. Amada, M. Tamura, Y. Nakagawa and K. Tomishige, *Green Chem.*, 2014, **16**, 617–626.
28 M. Hronec and K. Fulajtarová, *Catal. Commun.*, 2012, **24**, 100–104.
29 S. Bagheri, N. Muhd Julkapli and S. Bee Abd Hamid, *Sci. World*, 2014, **2014**, 727496.
30 M. Przydacz, M. Jędrzejczyk, M. Brzezińska, J. Rogowski, N. Keller and A. M. Ruppert, *J. Supercrit. Fluids*, 2020, **163**, 104827.
31 S. Chen, C. Ciotonea, K. De Oliveira Vigier, F. Jérôme, R. Wojcieszak, F. Dumeignil, E. Marceau and S. Royer, *ChemCatChem*, 2020, **12**, 2050–2059.
32 Z. Zhang, C. Liu, D. Liu, Y. Shang, X. Yin, P. Zhang, B. B. Mamba, A. T. Kuvarega and J. Gui, *J. Mater. Sci.*, 2020, **55**, 14179–14196.
33 X. Kong, R. Zheng, Y. Zhu, G. Ding, Y. Zhu and Y. W. Li, *Green Chem.*, 2015, **17**, 2504–2514.
34 H. Jia, Q. Lv, Q. Xia, W. Hu and Y. Wang, *Front. Chem.*, 2022, **10**, 979353.
35 M. Chatterjee, T. Ishizaka and H. Kawanami, *Green Chem.*, 2014, **16**, 4734–4739.
36 J. Mitra, X. Zhou and T. Rauchfuss, *Green Chem.*, 2015, **17**, 307–313.
37 D. Wu, S. Zhang, W. Y. Hernández, W. Baaziz, O. Ersen, M. Marinova, A. Y. Khodakov and V. V. Ordomsky, *ACS Catal.*, 2020, **11**, 19–30.
38 K. Tomishige, Y. Nakagawa and M. Tamura, *Green Chem.*, 2017, **19**, 2876–2924.
39 A. Turkin, S. Eyley, G. Preegel, W. Thielemans, E. Makshina and B. F. Sels, *ACS Catal.*, 2021, **11**, 9204–9209.
40 A. A Turkin, F. Rammal, S. Eyley, W. Thielemans, E. V. Makshina and B. F. Sels, *ACS Sustainable Chem. Eng.*, 2023, **11**, 8968–8977.
41 G. Bottari, A. J. Kumalaputri, K. K. Krawczyk, B. L. Feringa, H. J. Heeres and K. Barta, *ChemSusChem*, 2015, **8**, 1323–1327.
42 D. Gupta, R. Kumar and K. K. Pant, *Fuel*, 2020, **277**, 118111.
43 Y. B. Huang, M. Y. Chen, L. Yan, Q. X. Guo and Y. Fu, *ChemSusChem*, 2014, **7**, 1068–1072.
44 Q. Wang, J. Feng, L. Zheng, R. Bi, Y. He, H. Liu and D. Li, *ACS Catal.*, 2019, **10**, 1353–1365.
45 S. Li, M. Dong, M. Peng, Q. Mei, Y. Wang, J. Yang, Y. Y. Yang, B. Chen, S. Liu, D. Xiao, H. Liu, D. Ma and B. Han, *Innovation*, 2022, **3**, 100189.
46 A. Shivhare, A. Kumar and R. Srivastava, *ChemCatChem*, 2020, **13**, 59–80.
47 W. Fang and A. Riisager, *Green Chem.*, 2021, **23**, 670–688.
48 X. Chang, A. F. Liu, B. Cai, J. Y. Luo, H. Pan and Y. B. Huang, *ChemSusChem*, 2016, **9**, 3330–3337.
49 Z. Zhang, Z. Pei, H. Chen, K. Chen, Z. Hou, X. Lu, P. Ouyang and J. Fu, *Ind. Eng. Chem. Res.*, 2018, **57**, 4225–4230.
50 V. Oksanen, N. van Strien, T. Viertiö, N. Vuorio, B. Gauli, K. Helosuo, V. Meriläinen, E. Myllykylä, S. Rautiainen and T. Wirtanen, *ChemCatChem*, 2024, e202400422.
51 Z. Gao, C. Li, G. Fan, L. Yang and F. Li, *Appl. Catal., B*, 2018, **226**, 523–533.
52 J. C. Serrano-Ruiz, R. Luque, J. M. Campelo and A. A. Romero, *Challenges*, 2012, **3**, 114–132.
53 A. Hommes, H. J. Heeres and J. Yue, *ChemCatChem*, 2019, **11**, 4671–4708.
54 J. G. Stevens, R. A. Bourne, M. V. Twigg and M. Poliakoff, *Angew. Chem., Int. Ed.*, 2010, **49**, 8856–8859.
55 T. Wabnitz, D. Breuninger, J. Heimann, R. Backes and R. Pinkos, *US Pat.*, 8168807B2, 2012.
56 F. Dong, Y. Zhu, G. Ding, J. Cui, X. Li and Y. Li, *ChemSusChem*, 2015, **8**, 1534–1537.
57 P. Liu, L. Sun, X. Jia, C. Zhang, W. Zhang, Y. Song, H. Wang and C. Li, *Mol. Catal.*, 2020, **490**, 110951.
58 C. Wang, J. Luo, V. Liao, J. D. Lee, T. M. Onn, C. B. Murray and R. J. Gorte, *Catal. Today*, 2018, **302**, 73–79.

59 M. Kalong, W. Praikaew, S. Ratchahat, W. Chaiwat, W. Kooamornpattana, W. Klysubun, W. Limphirat, S. Assabumrungrat and A. Srifa, *Energy Fuels*, 2024, **38**, 9836.
60 J. Luo, L. Arroyo-Ramírez, J. Wei, H. Yun, C. B. Murray and R. J. Gorte, *Appl. Catal., A*, 2015, **508**, 86–93.
61 N. Viar, J. M. Requies, I. Agirre, A. Iriondo, M. Gil-Calvo and P. L. Arias, *ACS Sustainable Chem. Eng.*, 2020, **8**, 11183–11193.
62 N. Viar, M. Requies, I. Agirre, A. Iriondo, C. García-Sancho and P. L. Arias, *Energy*, 2022, **255**, 124437.
63 W. Yang and A. Sen, *US Pat.*, 20100307050A1, 2010.
64 W. Yang and A. Sen, *ChemSusChem*, 2010, **3**, 597–603.
65 Y. Peng, T. Li, X. Li, T. Gao and W. Yang, *Cellulose*, 2019, **26**, 8417–8428.
66 C. Li, H. Cai, B. Zhang, W. Li, G. Pei, T. Dai, A. Wang and T. Zhang, *Chin. J. Catal.*, 2015, **36**, 1638–1646.
67 M. A. Jackson, M. Appell and J. A. Blackburn, *Ind. Eng. Chem. Res.*, 2015, **54**, 7059–7066.
68 T. Li, S. S. G. Ong, J. Zhang, C. Jia, J. Sun, Y. Wang and H. Lin, *Catal. Today*, 2018, **339**, 296–304.